Metallomics

Accepted Manuscript

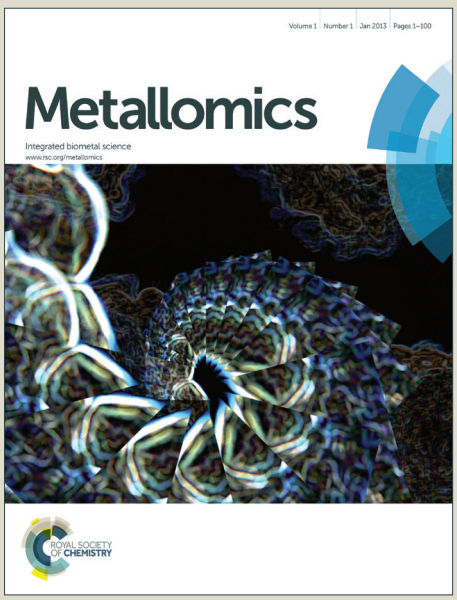

ROYAL SOCIETY OF CHEMISTRY

www.rsc.org/metallomics

Journal Name

RSCPublishing

ARTICLE

The Influence of Zinc(II) on Thioredoxin/Glutathione Disulfide Exchange: QM/MM Studies to Explore How Zinc(II) Accelerates Exchange in Higher Dielectric Environments

Cite this: DOI: 10.1039/xoxxoooooox

Received ooth January 2012,
Accepted ooth January 2012

DOI: 10.1039/xoxxoooooox

www.rsc.org/

Roby Kurian, Mitchell R. M. Bruce* Alice E. Bruce* and François G. Amar

QM/MM studies were performed to explore the energetics of exchange reactions of glutathione disulfide (GSSG) and the active site of thioredoxin [Cys32-Gly33-Pro34-Cys35] with and without zinc(II), in vacuum and solvated models. The activation energy for exchange, in the absence of zinc, is 29.7 kcal/mol for the solvated model. This is 3.3 kcal/mol higher than the activation energy for exchange in the gas phase, due to ground state stabilization of the active site Cys-32 thiolate in a polar environment. In the presence of zinc, the activation energy for exchange is 4.9 kcal/mol lower than in the absence of zinc (solvated models). The decrease in activation energy is attributed to stabilization of the charge-separated transition state, which has a 4-centered, cyclic arrangement of Zn--S--S--S with an estimated dipole moment of 4.2 D. A difference of 4.9 kcal/mol in activation energy would translate to an increase in rate by a factor of about 4000 for zinc-assisted thiol-disulfide exchange. The calculations are consistent with previously reported experimental results, which indicate that metal-thiolate, disulfide exchange rates increase as a function of solvent dielectric. This trend is opposite to that observed for the influence of the dielectric environment on the rate of thiol-disulfide exchange in the absence of metal. The results suggest a dynamic role for zinc in thiol-disulfide exchange reactions, involving accessible cysteine sites on proteins, which may contribute to redox regulation and mechanistic pathways during oxidative stress.

Introduction

Thiol-disulfide exchange reactions are critical for protein structure and cellular redox regulation.[1] The thioredoxin family of enzymes exploits thiol-disulfide exchange to achieve a variety of biological functions, ranging in reactivity from reduction, to oxidation, and isomerization.[2, 3] Proteins in the thioredoxin family are characterized by the presence of a structural motif called a 'thioredoxin fold' consisting of a four-stranded β-sheet, three flanking α-helices, and a highly conserved CXYC catalytic site, where C stands for cysteine and X and Y are two variable residues.[4, 5] Theoretical studies suggest that the range in reactivity across this family of enzymes is made possible by a delicate balance of electrostatic effects, which control the redox potential and nucleophilicity of the cysteines in the active site.[2]

Thioredoxin (Trx) is a cytoplasmic redox enzyme in the thioredoxin family, which is found in both eukaryotes and prokaryotes. Trx catalyzes the reduction of disulfide bonds in proteins and peptides, for example insulin,[4] and under some circumstances glutathione disulfide (GSSG).[6-8] As such it plays a key role in redox regulation and cell signalling, and also plays a role in various disease states, such as during oxidative stress-induced cancer.[9] Recent evidence also suggests that Trx can participate in metal binding and transport.[10-12] Thioredoxin activity is generally inhibited by transition metals, however, in a comparative experimental study involving many metals, zinc did not inhibit Trx activity.[13]

Zinc(II) is an essential transition metal that plays a structural and functional role in many proteins.[14] Zinc ions are at the borderline between hard and soft cations, and therefore can accommodate harder donors like oxygen and nitrogen, and also softer donors like sulfur. Sulfur coordination environments provide thermodynamic stability for zinc and at the same time, they allow kinetically fast ligand exchange. Thiolate ligands like cysteine permit reversible redox reactions with subsequent release and binding of zinc.[15] Although zinc(II) is redox inactive, coordination to sulfhydryl groups is an important aspect of the redox regulatory role of zinc in biology.[15] For example, under conditions of oxidative stress, zinc is released from metallothioneins (MT) and transferred to surface accessible sulfhydryl groups on proteins, one example being m-aconitase.[16] Release of zinc is proposed to occur via interactions of zinc-thiolate sites in MT with GSSG, which increases in concentration during oxidative stress.

An intriguing question is what is the advantage to the cell to have an increase in available zinc during oxidative stress?

Sulfydryl groups of proteins are exceptionally vulnerable to oxidation.[17] Maret and others suggest that through binding of zinc to surface accessible sulfydryl groups, zinc plays an important physiological role in the protection of thiols against irreversible oxidation.[18-20] There are a number of examples of thiol-containing proteins and enzymes which are protected by zinc, including Tubulin,[21] E. *coli* DNA topoisomerase I,[22] E. coli primase,[23] and the protein farmesyltransferase.[24]

We and others have shown that small molecule Zn(II)-thiolate model complexes are capable of mediating thiolate-disulfide exchange (eq 1).[25, 26] We have been interested in understanding the factors that influence this reaction, including the effect of solvent dielectric on the rate. Our experimental studies indicate that an increase in solvent dielectric leads to a large increase in rate (i.e. several orders of magnitude).[27] These results have potential biological relevance owing to that fact that the dielectric environment of proteins controls the rate of thiol-disulfide exchange reactions,[28] and that the influence of solvent dielectric on metal-thiolate disulfide exchange rates is opposite to that observed in the absence of metals, *i.e.*, thiol-disulfide exchange rates decrease with an increase in solvent dielectric.[29, 30]

$$S[ZnL_n] + R^*SSR^* \rightarrow R^*S[ZnL_n] + RSSR^* \qquad (1)$$

The hybrid quantum mechanical/molecular mechanics (QM/MM) calculations described in this paper are designed to explore the energetics of thiol-disulfide exchange of GSSG with the CGPC [Cys32-Gly33-Pro34-Cys35] active site of Trx, in the presence and absence of zinc, in vacuum and solvated model systems. The goals are (i) to explore whether zinc coordination to a cysteine-containing active site in a protein, which does not require a metal ion for activity, will alter the energetics of thiol-disulfide exchange and (ii) to determine whether the dielectric environment exerts a significant effect. Trx was selected owing to its key role in redox regulation of proteins via thiol-disulfide exchange, the availability of a crystal structure, and related theoretical studies by Ramos, et al. on the reaction of the CGPC active site of Trx (in the absence of metals) with the simple disulfide, CH_3SSCH_3.[31] We selected the more biologically relevant disulfide, GSSG, because of its role in release of zinc from MT during oxidative stress, as well as its role in glutathionylation, which serves to protect and provide redox regulation of reactive cysteines.[32-35] In addition, human thioredoxin has been observed to undergo glutathionylation when incubated with GSSG.[34] Reaction of Trx with GSSG may also occur in glutathione reductase-deficient cells, [6-8, 63] or under conditions of oxidative stress, which can increase the cellular concentration of GSSG. The dynamic role of zinc in cellular processes is receiving increasing attention,[36]and a better understanding of the implications of the interactions of "free" zinc ions with cysteine residues in proteins demands detailed studies.[37, 38] This work aims to explore how non-redox active zinc(II) can influence the redox activity of a CXYC active site.

The results for the exchange reaction of the CGPC active site of Trx with GSSG in the absence of zinc, in both vacuum and solvated models, will be described first. This is followed by a discussion of the exchange reaction in the presence of zinc, and concludes with a comparison of the energetics of thiol-disulfide exchange in the presence and absence of zinc.

Computational Methods

General Considerations

We selected the B3LYP functional and 6-31+G(d) basis set for DFT calculations based on consideration of a number of factors, including: structural information, suitability for different types of atoms involved (e.g. sulfur and zinc),[39-44] ease of convergence, and computational cost for a system with approximately 120 atoms. Hybrid meta DFT functionals and larger basis sets have become more widely available, and these have been shown to provide a better estimate of barrier heights than B3LYP.[45-48] However, since our focus was to understand the difference in structural parameters and energy barriers between two calculations, one with Zn(II) and one without Zn(II), we employed the B3LYP/6-31+G(d) as a starting point in exploration of these trends.

Full protein calculations

The interaction of the full protein with GSSG was calculated with a mixed quantum/classical approach.[49] The protein was initialized from the NMR structure of reduced thioredoxin (PDB entry 1XOB).[50] The entire protein structure was preoptimized at a molecular mechanics (MM) level of theory (UFF force field) and the resulting structure was used to prepare a hybrid QM/MM ONIOM input file which used parameters available in the Gaussian 09 program.[51] The active site residues [Cys32-Gly33-Pro34-Cys35] were selected for treatment at QM level of theory: the B3LYP [52-55] functional and 6-31+G(d) basis set were used for geometry optimizations. Glutathione disulfide was preoptimized using density functional theory, DFT (B3LYP/6-31+G(d)) and then, for the preparation of the reactant complex, the glycine and glutamic acid residues from GSSG (including the cysteine backbone) were shifted into the MM layer to minimize computational costs. Structural details of the reactant and product complexes were studied using the full protein structure of thioredoxin in the gas phase and all atoms were free to move in all stages of these ONIOM calculations. However, as we were unable to converge the transition states in the all-atom calculations, we clipped out the active site of the protein to do a calculation of the reaction pathway, including the transition state.

Active site calculations

After isolating the active site of the protein, we were able to calculate the transition state of this moiety to give insight into the kinetics of the reaction under different conditions. The active site was isolated by replacing the backbone bonds of the amino group of Cys-32 and the carboxylic acid group of Cys-35 with hydrogen atoms to maintain valency and the proton attached to the nucleophilic sulfur atom of Cys-32 was removed to generate the deprotonated thiolate. Both the active site of thioredoxin (which we will refer to as Trx(CGPC), and GSSG were pre-optimized and then combined to make the reactant complex. The glycine and glutamic acid residues from GSSG (including the cysteine backbone) were left in the MM layer (UFF force field). The active site residues, CGPC, the cysteine of GSSG, and the metal complex were defined in the quantum layer using the B3LYP functional. The 6-31+G(d) basis set was used for geometry optimizations of the combined reactant complex, frequency calculations, and intrinsic reaction coordinate (IRC) calculations. Both gas-phase and solvated

model calculations were performed, and solvation studies were done using the CPCM dielectric continuum model with water as solvent.[56, 57] Geometries for reactants and products for all mechanistic steps were located and characterized. Energy minimized reactants and products did not contain any imaginary frequencies.

Optimized reactants and products were used to locate the transition state (TS) structures for each mechanistic step, employing the *synchronous transit-guided quasi-Newton* (STQN) method implemented in Gaussian.[58, 59] This method is requested with the QST2 or QST3 option to the Opt keyword. The QST2 method requires two molecule specifications, optimized reactants and optimized products as inputs while the QST3 method requires an initial guess of the transition state structure in addition to the minimized reactants and products. The order of the atoms must be identical within all molecular specifications.

The free energy of activation was calculated by subtracting the sum of electronic and zero-point energies of the TS from that of the reactants. Atomic charges were calculated by Mulliken and natural population analysis (NBO) methods.

The energy minimized reactants and products were used to locate the transition state for selected reaction mechanisms. The transition states were successfully located using the QST3 method. The transition states found in gas phase reactions were used as the guess-transition state for the QST3 method for the solvated calculation. All stationary points were characterized by analyzing the number of imaginary frequencies through frequency calculations. Reactant and product minima contained no imaginary frequencies and all transition states located by using this method contained only one imaginary frequency.

Results and Discussion

Overview of thiol-disulfide exchange

The mechanism of thiol-disulfide exchange has been examined experimentally and theoretically.[28, 29, 31, 60-62] Experimental evidence and calculations are consistent with a rate-determining step involving deprotonation of thiol (eq. 2), generating a reactive thiolate which attacks disulfide, in an S_N2 manner, resulting in exchange (eq 3). The exchanged thiolate then picks up a proton (eq 4) to complete the exchange reaction (eq. 5). DFT studies by Ramos employing the simple model, CH_3S^- + CH_3SSCH_3, as well as the more realistic Trx enzyme active site-substrate model, $(CGPC)^-$ + CH_3SSCH_3, indicate that during exchange (eq. 3), the transition state occurs with a nearly linear arrangement of the three sulfur atoms.[31]

RSH			→	RS^-	+	H^+	(2)
RS^-	+	R*SSR*	→	RSSR*	+	$R*S^-$	(3)
$R*S^-$	+	H^+	→			R*SH	(4)
RSH	+	R*SSR*	→	RSSR*	+	R*SH	(5)

The mechanism for Trx-catalyzed redox reactions, first proposed by Holmgren,[5] parallels the more general mechanism of thiol-disulfide exchange. Deprotonation of the solvent-exposed Cys-32 creates a thiolate, which attacks the disulfide bond of a protein, forming a mixed disulfide. The second step involves deprotonation of the buried Cys-35, followed by nucleophilic attack on the intermediate mixed disulfide, leading to oxidized Trx and reduced dithiol protein. In our calculations, the first step involving exchange of GSSG with deprotonated Cys-32 in the CGPC active site in thioredoxin is investigated (eq 6). We designate the Trx active site as $Trx(\underline{C}GPC)^-$ with the underline indicating the site of Cys-32 deprotonation, i.e. $Trx(\underline{C}GPC)^-$, or position of the disulfide bond, i.e. (Trx(CGPC-SG).

$$Trx(\underline{C}GPC)^- + GSSG \rightarrow Trx(\underline{C}GPC\text{-}SG) + GS^- \quad (6)$$

Calculations to examine exchange in the absence of zinc (II)

Full protein calculations. Initially, we examined the unconstrained optimization of the protein/glutathione disulfide reactant complex. There are several local minima with different orientations of GSSG on the surface of the protein. The most stable orientation has one of the glycine residues of glutathione disulfide oriented away from the protein. Figure 1 shows the location (red outline) of the hydrophobic patch on the surface of thioredoxin in the thioredoxin, glutathione disulfide reactant complex. The hydrophobic part of the glutamic acid residue is oriented closer to the hydrophobic side chain of Ile-75, which appears to contribute to energy stabilization. In general, glutathione disulfide was found to be oriented away from the so-called hydrophobic patch on the surface of thioredoxin.[63] The hydrophobic patch is a 1,100 $Å^2$ area, containing 12 hydrophobic amino acids that have a role in substrate binding prior to reaction at the CGPC site.[64] The presence of the substrate (GSSG) did not result in any substantial changes in the protein active site. In particular, the S-S distance in the CGPC motif is 3.55 Å in the absence of substrate and 3.56 Å in the presence of GSSG.

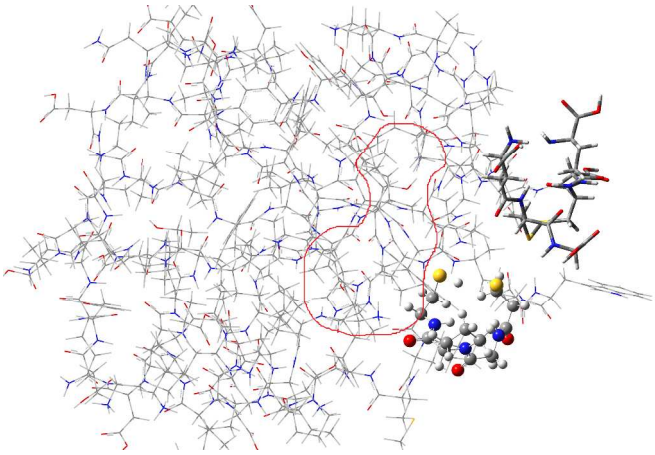

Fig.1 Approximate location of the hydrophobic patch (outlined in red) on the surface of thioredoxin in the thioredoxin/glutathione disulfide reactant complex. The portion of the active site of the protein treated in the QM layer is shown in ball-and-stick, while the GSSG is shown in a highlighted wireframe representation.

As per the study of Ramos,[31] we used the optimized configuration to model the enzyme-substrate interactions. The CGPC active site model of Trx was created by replacing the terminal points in the amino group of Cys-32 and carboxylic acid group of Cys-35 with hydrogen atoms. A comparison of the CGPC motif in the active site model and in the full protein in the gas phase shows similar conformations (see Fig. S9). The structure obtained by clipping out the active site was reoptimized with GSSG and used as the starting point in our calculations to model the reaction of glutathione disulfide with the active site of Trx, deprotonated at Cys-32 (i.e. glutathionylation, eq. 6).

Exchange reaction of $Trx(CGPC^-)$ active site with GSSG. Figure 2 shows the results of the solvated model calculation for the reactant complex and transition state for the reaction of the

Trx(CGPC$^-$) active site and glutathione disulfide. (Similar geometries were obtained in the vacuum and solvated models for the reactant complexes and transition states, respectively.) The Cys-32 sulfur is labeled S_n and the sulfurs in the disulfide are designated as central (S_c) and leaving (S_l). In the reactant complex (Fig. 2A), the S---S distance in the Trx(CGPC)$^-$ motif is 3.79Å and the S_n---S_c distance is 2.85Å. The two sulfur atoms of the disulfide substrate adopt a near linear orientation to the Cys-32 thiolate. (The S_n----S_c-S_l angle is 174.3°.) The reaction proceeds through a S_n--S_c--S_l transition state resulting from an S_N2@S nucleophilic attack by Cys-32 thiolate in the Trx(CGPC)$^-$ active site on the disulfide bond of the GSSG substrate (see Fig. 2B). The transition state geometry is similar to the transition state for the reaction of dimethydisulfide and CGPC$^-$ described by Ramos and coworkers,[31] but there are some significant differences. Specifically, in the transition state involving Trx(CGPC)$^-$ and GSSG, the angle between the three sulfur atoms is obtuse (at 139.2°) compared to the nearly linear transition state for reaction with dimethyl disulfide (178.5°). The sulfur-sulfur distances in the transition state (3.24 Å and 3.18 Å shown in Fig. 2B) are also longer than in the transition state previously reported (2.5 – 2.7 Å) by Ramos, et al.[31]

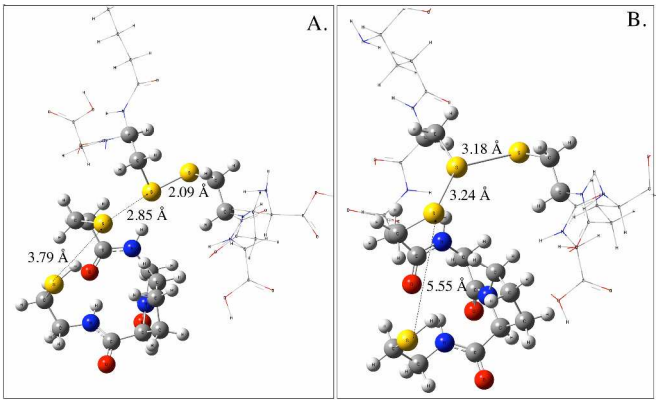

Fig. 2 Active site Trx(CGPC$^-$) model of the reaction of thioredoxin with glutathione disulfide (solvated model). QM layer shown as ball and stick; MM layer shown as wireframe. A. Reactant complex for Trx(CGPC$^-$) and GSSG. B. Transition state.

The energy diagrams for exchange between Trx(CGPC)$^-$ and GSSG are shown in Figure 3 for vacuum and solvated models. The solvated energy profile (reactant to product) is close to thermoneutral, while in the gas phase it is endothermic. In both cases, the reactant complexes are more stable than the separated reactants by approximately 0.7 kcal/mol (not shown in Figure 3). The activation barrier in the gas phase (26.4 kcal/mol) is similar to that found by Ramos, et al. for reaction of dimethyldisulfide with the CGPC active site of Trx$^-$ (25.3 kcal/mol with OPBE/TZ2P and 22.86 kcal/mol with BP86/TZ2P).[31]

The activation energy is higher (29.7 kcal/mol) in the solvated than in the vacuum model (26.4 kcal/mol). An increased activation barrier for the solvated system can be attributed to greater stabilization of the negatively charged thiolate ground state in a higher dielectric environment. Whereas in the transition state, the charge distribution on the S_n-S_c-S_l moiety is fairly symmetrical (i.e. -.21, -0.34 , -0.25, respectively) and would not be expected to experience significant stabilization in a higher dielectric environment. The central sulfur, which has a slightly higher negative charge density appears to be stabilized by hydrogen bonding involving the amide N-H groups of Gly-33 and the glycine in glutathione disulfide (not shown). As the reactant complex goes through the transition state to the product, the electron density on the nucleophilic sulfur (S_n) is gradually transferred to the leaving group sulfur (S_l). (see Fig S1-S3, showing the relative sizes of the orbitals centered on S_n, S_c and S_l, in the HOMOs and LUMOs for the reactant, transition state and product complexes.) To emphasize the stabilization of the ground state in the solvated model relative to the gas phase model, the transition state energies in Fig. 3A and 3B are set approximately equal.

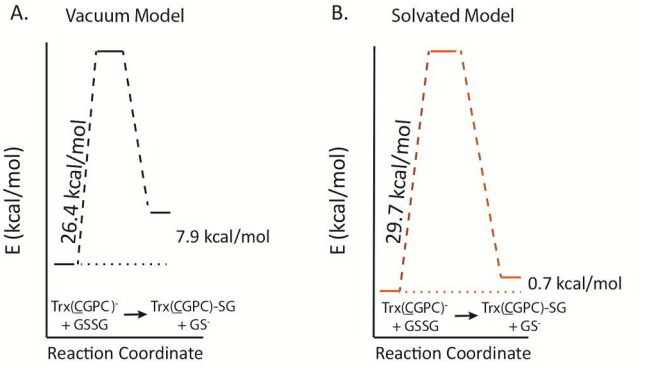

Fig. 3 Energy diagrams for the exchange reaction of Trx(CGPC)$^-$ and GSSG, in the absence of zinc(II), utilizing A. vacuum and B. solvated models. Note that while separated reactants and products are used to generate these values, the reactant complexes are slightly more stable than the separated reactants (by 0.7 kcal/mole in each case).

Calculations to examine exchange in the presence of zinc (II)

Full protein calculations. We next considered the question of how coordination of zinc to the Cys-32 sulfur in the CGPC active site of Trx alters the transition state and energetics of exchange with GSSG. Two neutral aqua ligands and a chloride ligand were coordinated to zinc(II) to form $[Zn(H_2O)_2Cl]^+$ and this complex was combined with the deprotonated form of thioredoxin (Trx$^-$) at the accessible Cys-32 sulfur, to form Trx-$Zn(H_2O)_2Cl$ (eq. 7). Initial attempts to carry out calculations with three water molecules in the coordination sphere, e.g. $[Zn(H_2O)_3]^{2+}$ failed to converge when locating the transition state. One water molecule was then replaced with an anionic chloride ligand in order to make the zinc-bound thioredoxin complex neutral and this choice permitted the calculation to converge. This structure was optimized using the Gaussian ONIOM method. The Zn-S bond distance is 2.21 Å, which is typical of Zn-S bonds in four coordinate zinc-thiolate complexes with approximately tetrahedral geometry. A Cambridge Structural Database search (accessed Dec 2014),[65] resulted in 132 four-coordinate Zn(II) complexes containing at least one oxygen donor and one terminal aliphatic or aromatic thiolate in which the average Zn-S bond length is 2.27 Å and the angles around Zn range from 82°-144°. The structural changes in the active site of thioredoxin as a result of zinc binding include loss of the hydrogen bond between the Cys-32 sulfur and the proton attached to the Cys-35 thiol. In addition, Cys-32 is more outwardly oriented as suggested by the substantial increase in the distance between the two sulfur atoms from 3.55 Å to 4.09 Å. This is expected to make the Cys-32 sulfur more accessible and interactions with an approaching substrate less sterically demanding. (Figure S4

shows the optimized geometries of the zinc-bound thioredoxin is included in the supporting information.)

$$[Zn(H_2O)_2Cl]^+ + Trx^- \rightarrow Trx\text{-}Zn(H_2O)_2Cl \quad (7)$$

Using the Gaussian ONIOM method, we evaluated two possible orientations of the GSSG substrate relative to the Cys-32 sulfur in Trx-zinc(II) thiolate. One was a parallel orientation, where the S-S bond of GSSG is approximately parallel to the S_n-Zn bond (dihedral angle of 6.46°) at a distance of 4.96 Å between the nucleophilic sulfur, S_n of Cys-32 and the nearest sulfur of GSSG. The other orientation was perpendicular, where the S-S bond of GSSG is approximately perpendicular to S_n-Zn bond (dihedral angle of 110.2°) at a distance of 4.96 Å between the nucleophilic sulfur, S_n of Cys-32 and the nearest sulfur of GSSG. These orientations are pictured in supporting information (see Figure S5) and were used to create Trx(CGPC)-Zn active site models to use in our calculations. In both of the parallel and perpendicular optimized structures, the orientation of GSSG is pointing away from the hydrophobic patch of thioredoxin.[64]

Exchange reaction of Trx(CGPC)-Zn active site with GSSG. Starting from the optimized full protein complexes, the active site model of Trx(CGPC)-$Zn(H_2O)_2Cl$ was created by replacing the terminal points in the amino group of Cys-32 and carboxylic acid group of Cys-35 with hydrogen atoms. The geometry about zinc remains approximately tetrahedral and the Zn-S bond distance (2.32Å) in the active site model is ca. 0.1 Å longer than in the full protein model. The exchange reaction was studied for the parallel and perpendicular orientations of GSSG in both gas and solvated phases (eq. 8).

$$Trx(CGPC)\text{-}Zn(H_2O)_2Cl + GSSG \rightarrow Trx(CGPC)\text{-}SG + GS\text{-}Zn(H_2O)_2Cl \quad (8)$$

The reactant complex with the perpendicular orientation of GSSG is more stable than the parallel orientation by about 6 kcal/mol. However, this structure does not lead to products.
The reasons for this may be due to steric hindrance caused by hydrogen bonding interactions between sulfur and H_2O ligands bound to zinc, or interactions between glycine carboxylic acid groups of GSSG and Glu-37 in Trx. The relative positions of active site residues are not affected by the presence of the GSSG substrate in the zinc-bound case as is evident from the distance between Cys-32 sulfur and Cys-35 sulfur, which remains unchanged at 4.09 Å, compared to the structure in the absence of substrate.

Figure 4 shows the results for the active site model of the reactant complex and transition state for the reaction of Trx(CGPC)-$Zn(H_2O)_2Cl$ and glutathione disulfide (solvated model). The reactant complex, shown in Figure 4A, has almost the same total energy as the initial structure with a parallel orientation of GSSG. However the dihedral angle between the S-S and the S_n-Zn(II) bond axes has increased from 6.46° to 45.6°, and now is in between a parallel and perpendicular orientation. In this rearranged reactant complex the distance between S_n of Cys-32 and the nearest sulfur of GSSG has decreased from 4.96 Å to 4.3 Å.

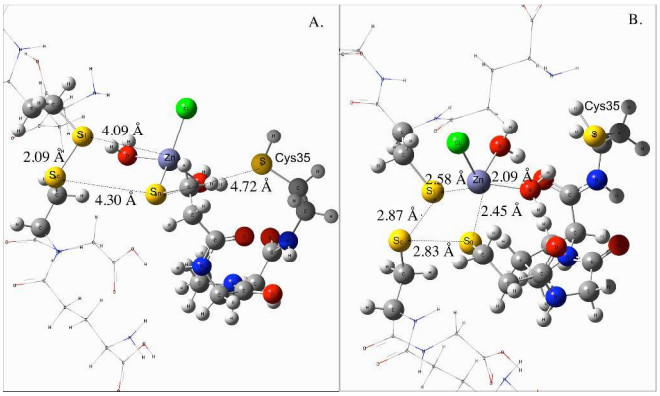

Fig. 4 Active site Trx(CGPC)-Zn model of the reaction of Trz-Zn with glutathione disulfide (solvated model). QM layer shown as ball and stick; MM layer shown as wireframe. A. Reactant complex for Trx(CGPC)-$Zn(H_2O)_2Cl$ and GSSG. B. Transition state.

In the transition state the three sulfurs and zinc atom adopt a cyclic geometry, in which the angle between the three sulfurs is acute (72.7°) and the zinc is positioned slightly above the plane formed by the three sulfurs (Figure 4B). The geometry approaches a square with an average bond length of 2.68 Å ± 0.2Å. The Zn-S_n bond (2.45 Å) is ca. 0.2 Å longer than in the reactants (2.27 Å) (not labeled in Figure 4a). The S-S distance in GSSG is longer in the transition state (2.87Å) than in the reactant complex (2.09Å) and the Zn-S_l distance is significantly shorter (2.58Å). Two waters and a chloride ligand are still coordinated to zinc in the transition state. The transition state illustrates the process of formation of a new disulfide bond between S_n and S_c, a new bond between Zn(II) and S_l, and weakening of the Zn(II)-S_n bond.

The energy diagrams for exchange between Trx(CGPC)-$Zn(H_2O)_2Cl$ and GSSG (eq 8) in vacuum and solvated models are shown in Figure 5. A significant finding is that the activation energy for exchange in the presence of zinc is lower in the solvated model (24.8 kcal/mol) than in the gas phase reaction (27.7 kcal/mol). This result is opposite to that seen for exchange in the absence of zinc (Fig. 3).

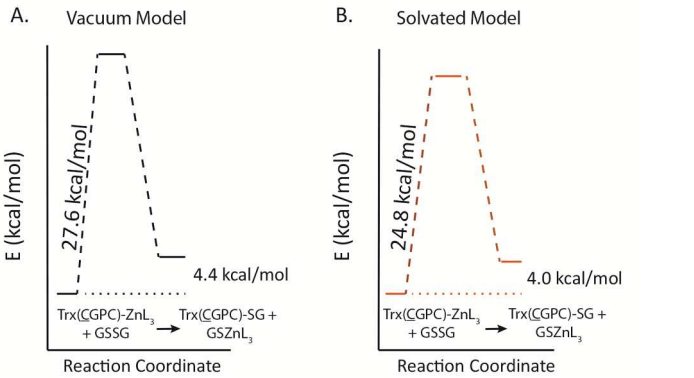

Figure 5. Energy diagrams for the exchange reaction of Trx(CGPC)-$Zn(H_2O)_2Cl$ and GSSG. A. Vacuum Model B. Solvated Model. As in the zinc-free case, reactant complexes are slightly more stable than the separated reactants shown here (by 1 kcal/mole and 0.5 kcal mole for cases vacuum and solvated models, respectively.

The influence of charge distributions on activation energies with and without zinc(II). Examination of the Mulliken charge distributions in the reactant complex and transition state (for the solvated model) provides insight into how zinc might affect the activation barrier. In the transition state, each of the sulfur atoms of

the S_n-S_c-S_l moiety has a partial negative charge: -0.23 on S_n, -0.344 on S_c, and -0.252 on S_l and zinc carries a positive charge (+0.74). While the charges on the sulfurs are fairly similar to that found in the transition state of the exchange reaction in the absence of zinc, the geometric arrangement combined with the positive charge on zinc significantly alters the charge distribution of the transition state.

The greater degree of charge separation in the transition in the presence of zinc than in the absence of zinc is illustrated by using a simple dipole approach.[66] Considering the atomic charges on each sulfur and the 140° angle between the sulfurs, a small dipole moment (μ), on the order of 0.2 D, is estimated for the transition state in the absence of zinc (Fig. 6A). This picture is qualitatively similar to the "classical" image of thiolate-disulfide exchange involving a highly symmetrical and fairly non-polar transition state. The consequence of bulky substituents on Trx(CGPC)$^-$ and GSSG appears to impose some deviation from this classical picture, but not significantly. Thus, the transition state is not significantly influenced when moving from lower to higher dielectric environments. Therefore, the driving force for changes to the energetics of the exchange reaction in vacuum vs. solvated models appears to be mainly from ground state stabilization of the free thiolate.[67]

A different picture emerges for the exchange reaction in the presence of zinc. The dipole moment for the transition state is estimated to be 4.2D (see Fig. 6B) based on the S---S and Zn---S distances (from Fig. 4B) and an idealized geometry (90° angles and co-planarity of the Zn-S-S-S moiety). In contrast, the dipole moment for the Zn-S_n bond in the reactant complex is estimated to be 2.7D (Zn: q=+0.75; S_n: q=-0.44; d=2.27Å from Fig. 4A). (The S-S bond in the disulfide is not included in the estimation of the dipole moment of the reactant complex because the disulfide is more than 4 Å away. This is beyond the sum of the van der Waals radii[68] for Zn-S (3.2Å) and S-S (3.6Å), indicating that these moieties do not interact in the reactant complex.) Thus, in the presence of zinc, the transition state, which has a greater degree of charge separation than the reactant complex, is expected to experience greater stabilization in a higher dielectric environment and therefore result in a lower activation energy relative to the vacuum model. We cannot exclude the possibility that stabilization may also originate from hydrogen bonding involving the amide oxygen of both Cys-32 and Pro-34 with two aqua ligands on zinc (not shown). To emphasize the stabilization of the transition state in the solvated model relative to the gas phase model, the reactant complex energies in Fig 5A and 5B are approximately equal.

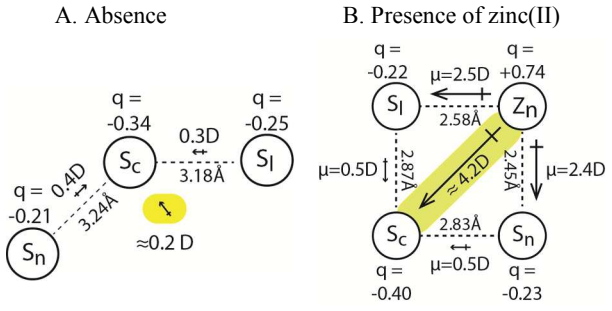

Figure 6. Cartoon drawings illustrating bond lengths, Mulliken charges, and estimates of dipole moments in the transition states involving: A. S-S-S and B. S-S-S-Zn moieties during the exchange of Trx(CGPC)$^-$ + GSSG in the absence and presence of zinc(II).

The influence of zinc(II) on exchange energetics

Comparison of exchange in the absence and presence of zinc(II). In the gas phase model, the presence of zinc(II) slightly increases the activation barrier for exchange (by 1.2 kcal/mol) relative to the exchange reaction in the absence of zinc (Fig. 5A vs Fig. 3A). In contrast, in the solvated model, the activation barrier is significantly lower in the presence of zinc. For the solvated model, this can be rationalized by considering the effects of ground and transition state energetics. For thiolate-disulfide exchange (i.e. the absence of zinc), the ground state is strongly stabilized by solvation owing to localized charge on the thiolate, while the more delocalized transition state is less influenced by solvation.[67] That is, for thiolate-disulfide exchange a larger activation barrier would lead to a decrease in rate as the dielectric constant of the solvent increases. This is consistent with experimental results, in which thiol-disulfide exchange is several orders of magnitude faster in solvents with low dielectric constants (e.g. CH_2Cl_2) than in water.[29] For zinc(II) thiolate, disulfide exchange, the opposite occurs. That is, the transition state, containing a four-centered cyclic structure that has significant charge separation involving zinc(II), Cys-32 sulfur of the Trx(CGPC) active site and the disulfide bond of glutathione disulfide, is expected to be more stabilized by solvation than the ground state zinc(II) thiolate. This combination of factors results in decreasing the activation barrier in the presence of zinc(II) for the solvated model by 4.9 kcal/mol. The decrease in activation energy would imply an increase in rate by a factor of about 4000 for zinc-assisted thiol-disulfide exchange. Recent experimental studies demonstrate that exchange reactions of small molecule zinc(II)-thiolate complexes and disulfides are faster in DMSO than in CH_2Cl_2.[27]

Speculations on the influence of zinc(II) on thiol-disulfide exchange. It has been generally accepted that glutathione disulfide and thioredoxin function independently in contributing to the maintenance of cellular redox balance. This assumption is reasonable owing to the fact that the reaction between Trx (thioredoxin-$(SH)_2$) and GSSG is much slower than for the corresponding Trx (thioredoxin-$(SH)_2$) and insulin disulfide reaction.[69, 70] The assumption may also be reasonable given that the level of GSSG in resting cells is low, where the ratio of GSH:GSSG can be on the order of 100:1.[1, 71] It is only in situations such as oxidative stress, where the GSH:GSSG ratio can decrease to 10:1 or below, that significant concentrations of GSSG approaching the millimolar level are produced.[72]

In a resting cell there is very low availability of zinc(II).[38] However, certain conditions are known to alter this low availability. For example, during physical and chemical stresses, metal trafficking can be disrupted,[73] and aging and chronic degenerative diseases are associated with the loss of zinc(II) homeostatic control.[74] Zinc(II) may also have potential beneficial effects on chronic inflammation,[75] and it has recently been suggested that during oxidative stress, zinc(II) release may trigger a mechanism to restore cellular thiol content, though the mechanism has not yet been elucidated.[76] The computational results reported here for the exchange reaction of GSSG and the Trx(CGPC) active site of Trx indicate that coordination of zinc to the solvent-exposed Cys-32 in Trx has the potential to alter the energetics of exchange in an aqueous environment by decreasing the activation barrier. The overall reaction would lead to a zinc-assisted glutathionylation reaction of Trx, thus protecting the protein from oxidative stress.

Conclusions

Hybrid QM/MM studies were performed to develop insight into the exchange reaction of GSSG with the active site CGPC (Cys-Gly-Pro-Cys) in Trx, in the presence and absence of zinc(II), in vacuum and solvated models. The B3LYP functional and 6-31+G(d) basis set were selected based on a number of factors that allowed convergence of the calculations to explore the influence of zinc(II) on thiolate disulfide exchange at a CXYC active site. While other basis sets and methodologies may be employed in future studies to provide better estimates of barrier heights, this study serves as a starting point to explore the effect of solvent dielectric on metal vs. nonmetal thiolate disulfide exchange. A key result is that the presence of zinc(II) significantly alters the transition state, forming a cyclic S-S-S-Zn moiety with a significant degree of charge separation, which is stabilized in higher dielectric environments. This results in a decrease in the activation barrier of 4.9 kcal/mol with respect to thiolate-disulfide exchange in the absence of zinc(II). The results help to explain experimental studies (reported elsewhere) which indicate that the reactions of $Tp^*Zn(SC_6H_4CH_3)$ and disulfides (e.g. $R=SC_6H_4NO_2$) occur faster in higher dielectric solvents. This trend is opposite to how the dielectric environment influences that rate of (non-metal) thiolate-disulfide exchange. The results suggest a dynamic role for zinc in thiol-disulfide exchange reactions, involving accessible cysteine sites on proteins, which may contribute to redox regulation and mechanistic pathways during oxidative stress.

Notes and references

University of Maine, Department of Chemistry, Orono, ME 04469 E-mail: mbruce@maine.edu, abruce@maine.edu; Fax +1-207-581-1191

Electronic Supplementary Information (ESI) available: Details of the calculations. See DOI: 10.1039/b000000x/

REFERENCES

1. H. F. Gilbert, in *Glutathione Centennial*, eds. N. Taniguchi, T. Higashi, Y. Sakamoto and A. Meister, Academic Press, San Diego, CA, Editon edn., 1989, pp. 73-87.
2. A. T. P. Carvalho, P. A. Fernandes, M. Swart, J. N. P. van Stralen, F. M. Bickelhaupt and M. J. Ramos, *J. Comput. Chem.*, 2009, **30**, 710-724.
3. E. S. J. Arner and A. Holmgren, *European Journal of Biochemistry*, 2000, **267**, 6102-6109.
4. A. Holmgren, *Journal of Biological Chemistry*, 1989, **264**, 13963-13966.
5. A. Holmgren, *Structure*, 1995, **3**, 239-243.
6. S. M. Kanzok, R. H. Schirmer, I. Turbachova, R. Iozef and K. Becker, *Journal of Biological Chemistry*, 2000, **275**, 40180-40186.
7. R. Bao, Y. Zhang, X. Lou, C.-Z. Zhou and Y. Chen, *BBA-Proteins Proteomics*, 2009, **1794**, 1218-1223.
8. Z. Cheng, L. D. Arscott, D. P. Ballou and C. H. Williams, Jr., *Biochemistry*, 2007, **46**, 7875-7885.
9. M. Valko, C. J. Rhodes, J. Moncol, M. Izakovic and M. Mazur, *Chem.-Biol. Interact.*, 2006, **160**, 1-40.
10. S. Quan, I. Schneider, J. Pan, A. Von Hacht and J. C. A. Bardwell, *Journal of Biological Chemistry*, 2007, **282**, 28823-28833.
11. S. Sitthisak, T. Kitti, K. Boonyonying, D. Wozniak, S. Mongkolsuk and R. K. Jayaswal, *FEMS Microbiol. Lett.*, 2012, **327**, 126-133.
12. S. Sitthisak, L. Knutsson, J. W. Webb and R. K. Jayaswal, *Microbiology-(UK)*, 2007, **153**, 4274-4283.
13. J. M. Hansen, H. Zhang and D. P. Jones, *Free Radical Biology and Medicine*, 2006, **40**, 138-145.
14. T. Kochanczyk, A. Drozd and A. Krezel, *Metallomics*, 2015, **7**, 244-257.
15. W. Maret and B. L. Vallee, *Proceedings of the National Academy of Sciences of the United States of America*, 1998, **95**, 3478-3482.
16. W. Feng, J. Cai, W. M. Pierce, R. B. Franklin, W. Maret, F. W. Benz and Y. J. Kang, *Biochem. Biophys. Res. Commun.*, 2005, **332**, 853-358.
17. A. J. Meyer and R. Hell, *Photosynthesis Research*, 2005, **86**, 435-457.
18. T. M. Bray and W. J. Bettger, *Free Radical Biology and Medicine*, 1990, **8**, 281-291.
19. W. Maret, *Neurochem. Int.*, 1995, **27**, 111- 117.
20. W. Feng, J. Cai, W. M. Pierce, R. B. Franklin, W. Maret, F. W. Benz and Y. J. Kang, *Biochem. Biophys. Res. Commun.*, 2005, **332**, 853-858.
21. J. E. Hesketh, *Int. J. Biochem.*, 1983, **15**, 743-746.
22. Y. C. Tsedinh and R. K. Beransteed, *Journal of Biological Chemistry*, 1988, **263**, 15857-15859.
23. M. A. Griep and E. R. Lokey, *Biochemistry*, 1996, **35**, 8260-8267.
24. H. W. Fu, J. F. Moomaw, C. R. Moomaw and P. J. Casey, *Journal of Biological Chemistry*, 1996, **271**, 28541-28548.
25. H. Boerzel, M. Koeckert, W. Bu, B. Spingler and S. J. Lippard, *Inorg. Chem.*, 2003, **42**, 1604-1615.
26. G. S. P. Garusinghe, S. M. Bessey, A. E. Bruce and M. R. M. Bruce, *Abstracts, 36th Northeast Regional Meeting of the American Chemical Society, Hartford, CT, United States, October 7-10*, 2009, NERM-285.
27. G. S. P. Garusinghe, Ph.D., University of Maine, 2013.
28. P. A. Fernandes and M. J. Ramos, *Chemistry - A European Journal*, 2004, **10**, 257-266.
29. R. Singh and G. M. Whitesides, *Journal of the American Chemical Society*, 1990, **112**, 1190-1197.
30. P. A. Fernandes and M. J. Ramos, *Chemistry-A European Journal*, 2004, **10**, 257-266.
31. A. T. P. Carvalho, M. Swart, J. N. P. van Stralen, P. A. Fernandes, M. J. Ramos and F. M. Bickelhaupt, *Journal of Physical Chemistry B*, 2008, **112**, 2511-2523.
32. M. Zaffagnini, M. Bedhomme, C. H. Marchand, J. Couturier, X.-H. Gao, N. Rouhier, P. Trost and S. D. Lemaire, *Antioxidants & Redox Signaling*, 2012, **16**, 17-32.
33. M. M. Gallogly and J. J. Mieyal, *Current Opinion in Pharmacology*, 2007, **7**, 381-391.
34. S. Casagrande, V. Bonetto, M. Fratelli, E. Gianazza, I. Eberini, T. Massignan, M. Salmona, G. Chang, A. Holmgren and P. Ghezzi, *Proceedings of the National Academy of Sciences of the United States of America*, 2002, **99**, 9745-9749.
35. D. M. Townsend, *Mol. Interv.*, 2007, **7**, 313-324.
36. A. G. Daniel and N. P. Farrell, *Metallomics*, 2014, **6**, 2230-2241.
37. N. M. Giles, A. B. Watts, G. I. Giles, F. H. Fry, J. A. Littlechild and C. Jacob, *Chemistry & Biology*, 2003, **10**, 677-693.
38. W. Maret, *Metallomics*, 2015, **7**, 202-211.
39. L. Lin, B. S. Peng, W. Y. Shi, Y. Y. Guo and R. J. Li, *Dalton Transactions*, 2015, **44**, 5867-5874.
40. K. Kaur, S. Chaudhary, S. Singh and S. K. Mehta, *J. Lumin.*, 2015, **160**, 282-288.
41. S. F. Sousa, E. S. Carvalho, D. M. Ferreira, I. S. Tavares, P. A. Fernandes, M. J. Ramos and J. Gomes, *J. Comput. Chem.*, 2009, **30**, 2752-2763.
42. S. F. Sousa, P. A. Fernandes and M. J. Ramos, *Journal of Physical Chemistry B*, 2007, **111**, 9146-9152.
43. E. I. Solomon, S. I. Gorelsky and A. Dey, *J. Comput. Chem.*, 2006, **27**, 1415-1428.
44. P. A. Denis, *J. Chem. Theory Comput.*, 2005, **1**, 900-907.
45. Y. Zhao, N. Gonzalez-Garcia and D. G. Truhlar, *Journal of Physical Chemistry A*, 2006, **110**, 4942-4942.

46. E. A. Amin and D. G. Truhlar, *J. Chem. Theory Comput.*, 2008, **4**, 75-85.
47. N. Kumar, M. Alfonso-Prieto, C. Rovira, P. Lodowski, M. Jaworska and P. M. Kozlowski, *J. Chem. Theory Comput.*, 2011, **7**, 1541-1551.
48. N. Kumar, M. Jaworska, P. Lodowski, M. Kumar and P. M. Kozlowski, *Journal of Physical Chemistry B*, 2011, **115**, 6722-6731.
49. T. Vreven, B. Mennucci, C. O. da Silva, K. Morokuma and J. Tomasi, *Journal of Chemical Physics*, 2001, **115**, 62-72.
50. M. F. Jeng, A. P. Campbell, T. Begley, A. Holmgren, D. A. Case, P. E. Wright and H. J. Dyson, *Structure*, 1994, **2**, 853\-868\.
51. G. W. T. M. J. Frisch, H. B. Schlegel, G. E. Scuseria, M. A. Robb, J. R. Cheeseman, G. Scalmani, V. Barone, B. Mennucci, ; G. A. Petersson, H. N., M. Caricato, X. Li, H. P. Hratchian, A. F. Izmaylov, J. Bloino, G. Zheng, J. L. Sonnenberg, M. Hada, M. Ehara, K. Toyota, R. Fukuda, J. Hasegawa, M. Ishida, T. Nakajima, Y. Honda, O. Kitao, H. Nakai, T. Vreven, J. A. Montgomery, Jr., J. E. Peralta, F. Ogliaro, M. Bearpark, J. J. Heyd, E. Brothers, K. N. Kudin, V. N. Staroverov, R. Kobayashi, J. Normand, K. Raghavachari, A. Rendell, J. C. Burant, S. S. Iyengar, J. Tomasi, M. Cossi, N. Rega, J. M. Millam, M. Klene, J. E. Knox, J. B. Cross, V. Bakken, C. Adamo, J. Jaramillo, R. Gomperts, R. E. Stratmann, O. Yazyev, A. J. Austin, R. Cammi, C. Pomelli, J. W. Ochterski, R. L. Martin, K. Morokuma, V. G. Zakrzewski, G. A. Voth, P. Salvador, J. J. Dannenberg, S. Dapprich, A. D. Daniels, O. Farkas, J. B. Foresman, J. V. Ortiz, J. Cioslowski, and D. J. Fox, Editon edn., 2009.
52. A. D. Becke, *Journal of Chemical Physics*, 1993, **98**, 5648-5652.
53. C. T. Lee, W. T. Yang and R. G. Parr, *Physical Review B*, 1988, **37**, 785-789.
54. S. H. Vosko, L. Wilk and M. Nusair, *Can. J. Phys.*, 1980, **58**, 1200-1211.
55. P. J. Stephens, F. J. Devlin, C. F. Chabalowski and M. J. Frisch, *Journal of Physical Chemistry*, 1994, **98**, 11623-11627.
56. V. Barone and M. Cossi, *Journal of Physical Chemistry A*, 1998, **102**, 1995-2001.
57. M. Cossi, N. Rega, G. Scalmani and V. Barone, *J. Comput. Chem.*, 2003, **24**, 669-681.
58. C. Y. Peng and H. B. Schlegel, *Isr. J. Chem.*, 1993, **33**, 449-454.
59. C. Y. Peng, P. Y. Ayala, H. B. Schlegel and M. J. Frisch, *J. Comput. Chem.*, 1996, **17**, 49-56.
60. G. M. Whitesides, J. E. Lilburn and R. P. Szajewski, *Journal of Organic Chemistry*, 1977, **42**, 332-338.
61. Z. Shaked, R. P. Szajewski and G. M. Whitesides, *Biochemistry*, 1980, **19**, 4156-4166.
62. G. M. Whitesides, J. Houk and M. A. K. Patterson, *Journal of Organic Chemistry*, 1983, **48**, 112-115.
63. H. Eklund, C. Cambillau, B. M. Sjoberg, A. Holmgren, H. Jornvall, J. O. Hoog and C. I. Branden, *EMBO J.*, 1984, **3**, 1443-1449.
64. G. Powis, D. Mustacich and A. Coon, *Free Radical Biology and Medicine*, 2000, **29**, 312-322.
65. F. Allen, *Acta Crystallographica Section B*, 2002, **58**, 380-388.
66. T. D. Gierke, H. L. Tigelaar and W. H. Flygare, *Journal of the American Chemical Society*, 1972, **94**, 330-&.
67. R. Singh and G. M. Whitesides, *Chemistry of Sulphur-Containing Functional Groups*, 1993, 633-658.
68. A. Bondi, *Journal of Physical Chemistry*, 1964, **68**, 441-&.
69. D. Nikitovic and A. Holmgren, *Journal of Biological Chemistry*, 1996, **271**, 19180-19185.
70. A. Holmgren, *Annu. Rev. Biochem.*, 1985, **54**, 237-271.
71. O. Zitka, S. Skalickova, J. Gumulec, M. Masarik, V. Adam, J. Hubalek, L. Trnkova, J. Kruseova, T. Eckschlager and R. Kizek, *Oncology Letters*, 2012, **4**, 1247-1253.
72. H. F. Gilbert, in *Bioelectrochemistry of Biomacromolecules*, eds. G. Lenaz and G. Milazzo, Birhäuser Verlag, Basel, Boston, and Berlin, Editon edn., 1997, vol. 5, pp. 256-324.
73. L. A. Finney and T. V. O'Halloran, *Science*, 2003, **300**, 931-936.
74. W. Maret, *Experimental Gerontology*, 2008, **43**, 363-369.
75. A. S. Prasad, *Curr. Opin. Clin. Nutr. Metab. Care*, 2009, **12**, 646-652.
76. A. Kinazaki, H. Chen, K. Koizumi, T. Kawanai, T. Oyama, M. Satoh, S. Ishida, Y. Okano and Y. Oyama, *J Physiol Sci*, 2011, **61**, 403-409.